Catalysis Science & Technology

ROYAL SOCIETY OF CHEMISTRY

PAPER

View Article Online
View Journal | View Issue

Cite this: *Catal. Sci. Technol.*, 2024, 14, 6298

Directed evolution of C-methyltransferase PsmD for enantioselective pyrroloindole derivative production†

Diana A. Amariei,[a] Julia Tenhaef,[b] Thomas Classen,[b] Benoit David,[c] Tobias M. Rosch,[b] Holger Gohlke,[cd] Stephan Noack[b] and Jörg Pietruszka *[ab]

Received 23rd May 2024,
Accepted 5th September 2024

DOI: 10.1039/d4cy00657g

rsc.li/catalysis

The natural product physostigmine is known for its capacity to inhibit acetylcholinesterase (AChE). The pyrroloindole-based scaffold of physostigmine is prevalent among various compounds demonstrating AChE inhibition, suggesting that its structural diversification holds promise as a strategy for the development of novel AChE inhibitors. The C-methyltransferase PsmD is involved in the biosynthesis of physostigmine. While the two described variants from *Streptomyces griseofuscus* and *Streptomyces albulus* display an extended substrate range, their specificity hinders the efficient methylation of substrate derivatives. In order to improve the activity of PsmD towards voluminous non-natural substrates, we employed an iterative saturation mutagenesis strategy, which led to an increase in the available space in the catalytic site, while maintaining stereoselectivity. To aid our efforts and provide an efficient platform for the evolution of pyrroloindole-forming enzymes, we developed a modular automated process for the expression, enzymatic reaction and activity screening of the obtained mutant libraries, using an integrated robotic system. In this way, we identified multiple mutants, which led to increased specific activity towards our target substrates. Our results enabled the identification of amino acid position 166 as a key site for the modulation of substrate specificity. We immobilized the best mutant W166C, and used it for the preparative synthesis of an AChE inhibitor, in the presence of a SAM cofactor recycling system.

Introduction

The pyrroloindole scaffold is present in multiple compounds known to exhibit acetylcholinesterase (AChE) inhibition, some of which are approved drugs against Alzheimer's disease, glaucoma or cholinergic poisoning.[1–7] Physostigmine is one of the most well-known compounds in this class and several of its analogs were also found to exhibit AChE and butyrylcholinesterase (BChE) inhibition (Fig. 1).[8] Other drugs and natural products containing the 1,2,3,3*a*,8,8*a*-hexahydropyrrolo[2,3-*b*]indole (pyrroloindole) motif show a variety of therapeutic effects, ranging from analgesics to antibiotics or tumor suppressants.[9–11] The structural diversification of this scaffold could provide a path to new drugs, and the possibility to improve the pharmacological properties of the existing ones. For this reason, multiple chemical routes have been developed for the synthesis of these compounds. While in some cases the methylation of the indole leads to a racemic mixture, which then needs to be separated, asymmetric synthesis methods were also developed using chiral catalysts to introduce the stereogenic center earlier in the sequence.[12–17] An enzymatic route towards these compounds can be attractive in particular due to the late-stage enantioselective introduction of the stereogenic center on the indole ring.[18] The biosynthetic pathway of physostigmine has been elucidated and it revealed that a C-methylation step on a tryptophan metabolite is responsible for the chirality of the natural product (Scheme 1).[19] The responsible methyltransferase, PsmD, has been characterized and a more stable homolog has been identified and used in preparative enantioselective methylation in the 3-position.[8,20] In our previous work, we obtained the crystal structure of PsmD from *S. griseofuscus* (PsmD_*Sg*), mapped the catalytic site and identified the amino acid residues that are essential for the enzymatic activity.[20] We also assessed the activity of PsmD

[a] *Institute of Bioorganic Chemistry & Bioeconomy Science Center (BioSC), Heinrich Heine University Düsseldorf in Forschungszentrum Jülich, Jülich, Germany. E-mail: j.pietruszka@fz-juelich.de*
[b] *Institute of Bio- and Geosciences (IBG-1: Biotechnology), Forschungszentrum Jülich, Jülich, Germany*
[c] *Institute of Bio- and Geosciences (IBG-4: Bioinformatics), Forschungszentrum Jülich, Jülich, Germany*
[d] *Institute for Pharmaceutical and Medicinal Chemistry & Bioeconomy Science Center (BioSC), Heinrich Heine University Düsseldorf, Düsseldorf, Germany*
† Electronic supplementary information (ESI) available. See DOI: https://doi.org/10.1039/d4cy00657g

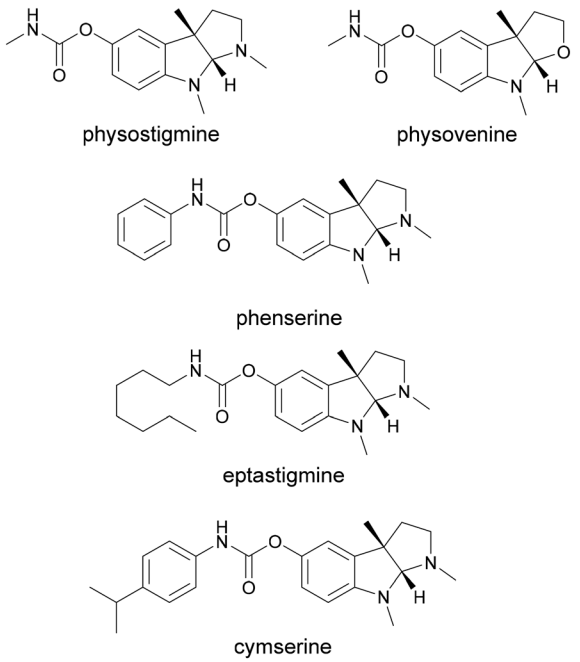

Fig. 1 Known biologically active compounds sharing the physostigmine scaffold.

towards other derivatives of the natural substrate. Based on this information, in the work presented here, we attempted to evolve the enzyme in order to increase activity towards a larger variety of substrates while maintaining stereoselectivity. Most enzymes, in particular those belonging to secondary metabolism are not performant enough for preparative approaches and less so for economically viable industrial processes.[21,22] Enzyme engineering is now a firmly established procedure for the improvement of catalytic properties.[23] There are multiple paths such as rational and computational design, semi-rational design or directed evolution.

While the rational approach is more accessible experimentally, it requires detailed structural and mechanistic knowledge in order to accurately predict the optimal mutations. Directed evolution eliminates bias and greatly expands the possibility of favorable outcomes but requires extensive library generation and screening efforts. In many cases, a middle ground is the preferred choice, having a semi-rational approach while still maintaining some degree of randomness. This generates focused mutant libraries, significantly reducing the screening efforts.[24–27] Small molecule methyltransferases have attracted attention as synthetic options for complex methylated compounds, due to their chemo-, regio- and stereoselectivity.[28–32] Several of these enzymes have found their way into the synthesis and diversification of clinically relevant natural products.[33–40] The engineering of natural product methyltransferases can be challenging, due to the low reaction rates, limited availability of substrates and the currently limited number of identified and characterized enzymes in this class.[29] The necessity of the SAM cofactor in stoichiometric amounts is also a significant barrier to extensive screening efforts due to its price and chemical lability.

Several SAM recycling systems have been recently developed offering much-needed solutions to the cofactor issue when it comes to preparative and industrial applications.[41–45] Nevertheless, the recent advances in this line of study have produced several very successful examples of methyltransferase engineering in the last years.[46–52] A 235-fold improvement in the total turnover number was achieved for the methylation of α-keto acids by engineering the C-methyltransferase SgvM, while the engineering of human NMT produced up to 118-fold increase in activity for the N-methylation of pyrazoles.[53,54] This indicates the potential for the evolution of small molecule methyltransferases, albeit the practical implementation is still in its early stage. In this work, we modified the C-methyltransferase PsmD from *S. albulus* (PsmD_*Sa*, the organism of origin also recently annotated as *Streptomyces noursei*) in order to expand its substrate scope, while maintaining stereoselectivity.[55] We used a semi-rational design approach by performing saturation mutagenesis on selected residues in the catalytic site and we developed an automated screening strategy for the obtained mutant libraries. In this way, we could identify variants displaying increased activity for larger substrates, and use them in combination with a cofactor recycling system for the preparative synthesis of physostigmine analogs.

Results and discussion

Mutagenesis targets

We chose two model substrates for our screening efforts. Although multiple physostigmine analogues present structural diversity on the carbamate moiety, diversification of the amide was scarcely explored.[56] For this reason, we chose compound **2a** as a substrate, containing a *t*-butyl residue which adds

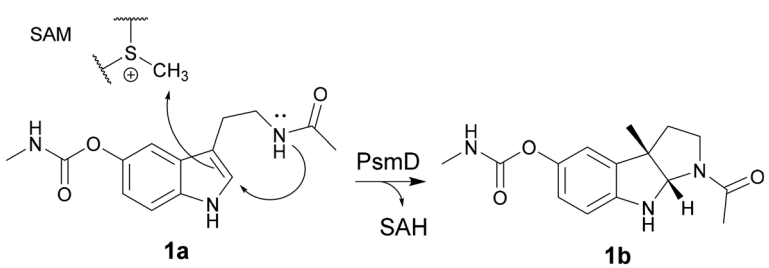

Scheme 1 Reaction catalyzed by PsmD, the natural substrate (**1a**) and product (**1b**).

considerable extra volume to the molecule and was found to exhibit significant AChE and BChE inhibitory effects.[8] Conversely, we also explored the use of **3a** as a substrate for mutant libraries, with the aim of obtaining a precursor of the AChE inhibitor phenserine, which is not produced naturally (Fig. 2A).[57] After site-directed mutagenesis to alanine or phenylalanine to assess the importance of the amino acids lining the catalytic pocket, we chose positions that can sterically hinder the binding of larger substrates, but do not affect the catalytic process (Table S2†). Our previous computational simulations revealed two possible positions of the substrate in the catalytic pocket.[20]

Due to the loss of activity upon replacement of the Glu-His-Tyr catalytic triad, we expected the pose in which the indole amine is oriented towards Y128 (Fig. 2C and D) to be productive for methylation.[20] We chose two voluminous residues on each side of the docked substrate as saturation mutagenesis positions: W33 and W166, which are part of a previously observed Trp cluster lining the back of the catalytic pocket, and Y197 and Y15 from the lid region (Fig. 2B–D).[20] The aromatic

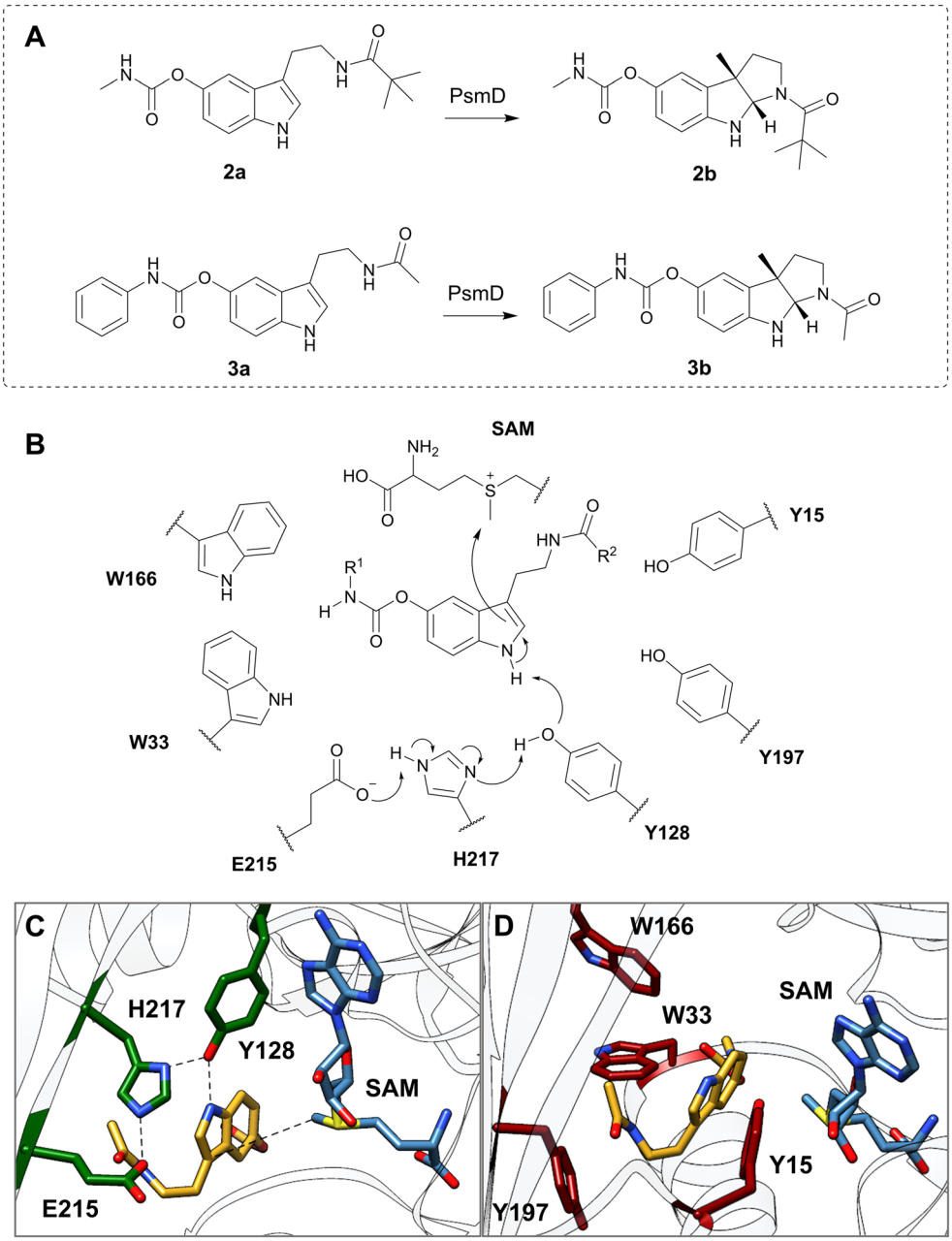

Fig. 2 A. Substrates used for the mutant library screening. B. Scheme of the catalytic mechanism and the positions of the chosen amino acids relative to the substrate in the catalytic site. C. Catalytic site of PsmD with SAM (blue) and the docked substrate (yellow). The Glu-His-Tyr catalytic triad is highlighted in green. D. Catalytic site of PsmD with SAM (blue) and the docked substrate (yellow). The residues chosen for saturation mutagenesis are highlighted in red.

residues are not highly conserved in the sequences of similar methyltransferases, suggesting the evolutionary variability of these positions (Fig. S7†). Due to the high metabolic price for incorporating tryptophan in protein sequences, the presence of four tryptophans (W33, W166, W171 and W182) in this region of the catalytic pocket is likely important for the substrate specificity (Fig. S13†).[58] A "compression" motion within the catalytic site of methyltransferases was suggested to promote the enzymatic S_N2-type methylation, by reducing the energy barrier to the transition state.[59–62] This offers a plausible explanation for the two observed conformations (open and closed) of PsmD. It was found that the closure of the lid influences the conformation of the cofactor and reduces the available space. In this context, we aimed to reduce the steric constraints in the catalytic pocket as much as possible, while maintaining a compact space to enable methylation.

Mutant library production

The mutant libraries were generated using the 22c trick, which allows for a reduction of codon redundancies while maintaining full variance of amino acids, consequently reducing the screening resources.[63] As such, degenerated primer mixtures were used to introduce mutations to all 20 amino acids in each position. 66 colonies were selected from each library to probably represent all 20 amino acids. *E. coli* BL21 Gold(DE3) cells were transformed with the obtained plasmid mixtures and the obtained agar plates were used directly in the automated process.

Process design

The library screening process involved multiple process steps and was divided into three main modules comprising the protein expression, the enzymatic reaction and the activity assay (Fig. 3). To increase reproducibility and consistency across multiple libraries, we used an automated approach for all modules. This also enabled easy adaptation and extension of the process for further enzymes or different assay conditions. The automated sequence started with colony picking, followed by two consecutive cultivation steps during which the enzymes were expressed using autoinduction. The liquid handling, plate transport, centrifugation, mixing and incubation steps were performed using the integrated AutoBioTech laboratory platform.[64] The membrane permeability of the PsmD substrates and products allowed us to perform the enzymatic reactions using whole-cell systems. To screen for activity, a modified version of our previously described indole assay was used, which utilizes *p*-dimethylaminobenzaldehyde (DMAB) and H_2SO_4 to form colored products with the indole ring of the substrate (Fig. 4).[65] The absorbance at 580 nm was measured and heatmaps were created in order to select the positions with the highest substrate consumption. The system allowed the processing of up to four plates in parallel and provided an almost complete removal of human experimental input.

Library screening using substrate 2a

After identification of the mutants, the hits of each round were isolated and their specific activity was determined.

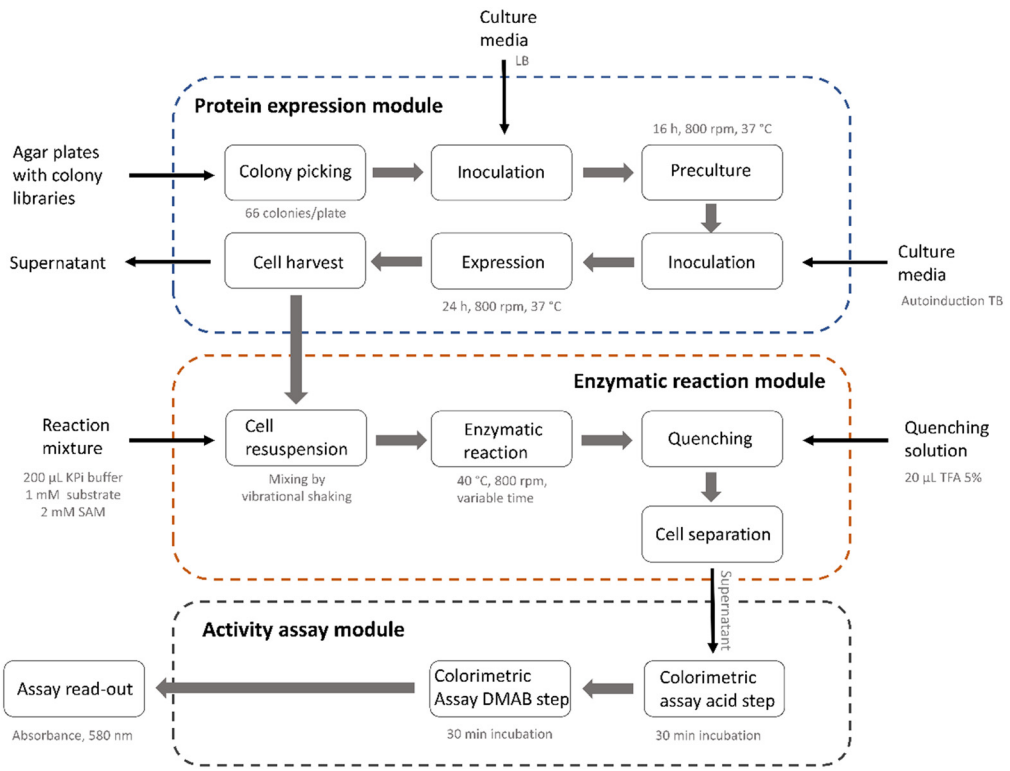

Fig. 3 Operation scheme of the automated screening process using the AutoBioTech platform.

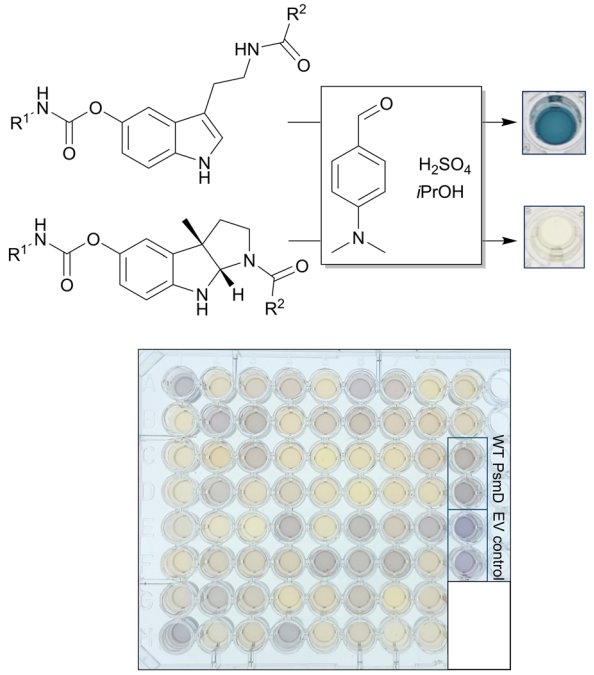

Fig. 4 Scheme of the colorimetric assay used for the detection of the substrate indole and example of a library plate after the assay. EV refers to the "empty vector" negative control.

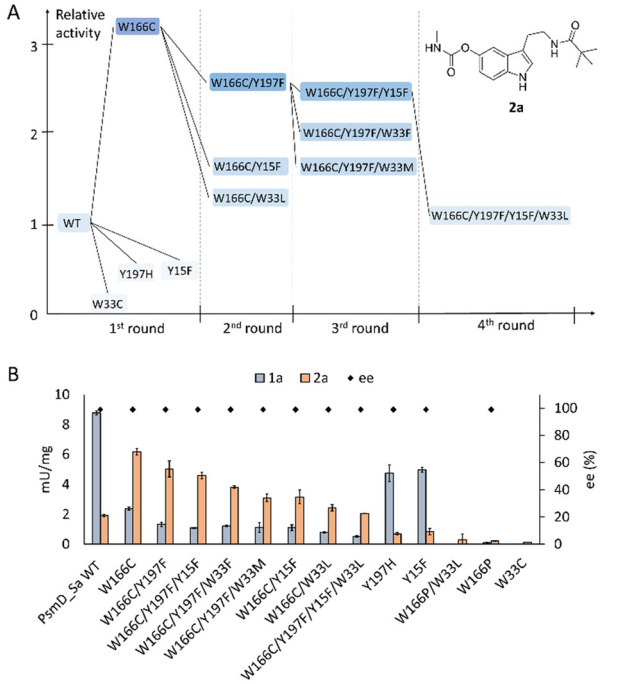

Fig. 5 A. Hits from every round of mutagenesis and screening using **2a** as a substrate and their activity relative to WT PsmD. B. Specific activities of all the hits from the screening experiments for the natural substrate **1a** (blue) and the selected substrate **2a** (orange) as well as the enantiomeric excess for reactions with **2a** (diamond shape). The specific activities were determined using the commercial MTase-Glo™ assay. In the case of W33C and W166P/W33L, the enantiomeric excess could not be determined.

Interestingly, position W166 turned out to be the most versatile, leading to the best hits for both **2a** and **3a**. Replacing the tryptophan in this position with a cysteine led to a three-fold increase in the specific activity towards **2a**, compared to the wild type (Fig. 5A). The best hits containing new mutations in each library were used as parents for subsequent mutagenesis rounds, in the hope of identifying cooperative effects of multiple mutations.

Unfortunately, this was not the case, as further mutagenesis rounds did not improve the performance beyond mutant W166C. Most mutants did however keep an increased activity towards this substrate, when compared to the wild type. As we expected, increasing the space in the catalytic site drives an improvement in the acceptance of the bulkier **2a** containing the *t*-butyl amide, at the expense of the activity towards the natural substrate (Fig. 5B). Indeed, the degree of freedom added to the natural substrate within the modified catalytic site can hinder its binding in a productive position for methylation. The reduced activity of the single mutants in the positions Y15, Y197 and W33 suggests that further optimization in these positions is not beneficial for the tested substrates. All active mutants maintained the stereoselectivity of the transformation to **2b** (Fig. 5B). The structural explanation for the importance of position W166 was found by docking the respective substrates into the homology model of PsmD_*Sa*. We used the homolog PsmD_*Sg*, for which X-ray structures are available (PDB ID: 7ZKH, 7ZGT, 7ZKG), as a template for the homology model generation with MODELLER.[66] Two protein forms were identified upon crystallization, determined by the movement of an N-terminal "lid".

Our previous mechanistic analysis suggests that the closed conformation is active, therefore it was selected for the generation of the PsmD_*Sa* homology model and the docking experiments. An extensive probing of the active site of WT PsmD_*Sa* and the W166C variant was performed using molecular docking of the substrate **2a**. Several thousands of poses were obtained for each enzyme-substrate combination, which were then subjected to principal component analysis, to reveal the most probable productive configuration of substrate **2a** in the catalytic site. The data was then analyzed in regards to binding energy and distance between the cofactor and the methylation site. Our previous mechanistic study of PsmD revealed the productive binding mode of the natural substrate **1a** (Fig. 2C and D). This overlaps with one of the pose clusters obtained after docking substrate **2a** in both variants (cluster 6, Fig. S2 and S3†). However, the cluster occupation differs significantly between WT PsmD and mutant W166C (Fig. 6). The productive binding mode was markedly more likely to occur among the docking results of W166C than WT PsmD. This is in accord with the observed activity difference between the two variants, confirming our choice of pose as the most probable active configuration of the substrate **2a** in the catalytic site of PsmD.

The comparison between the docked substrate **2a** in WT PsmD_*Sa* and mutant W166C shows that a gap forms between the residues in the positions 166 and 33 (Fig. 6).

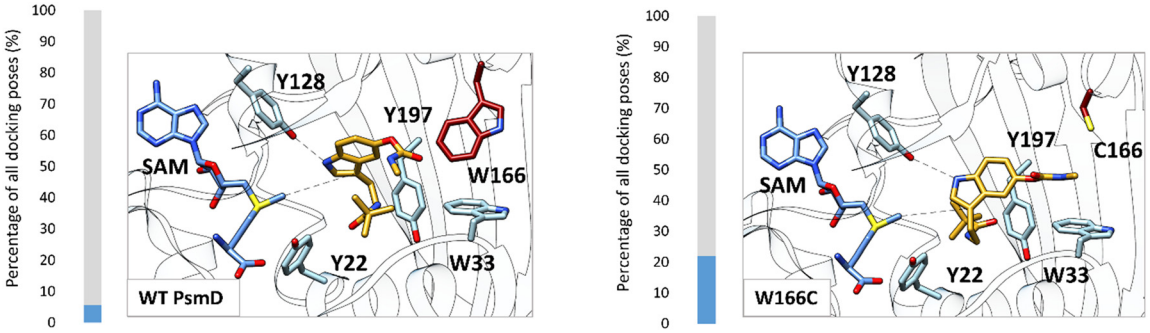

Fig. 6 Comparison of the active pose of docked substrate **2a** in the catalytic pocket of WT PsmD and the mutant W166C. The proportion of the active binding mode in all the obtained docking poses is represented as percentages (blue). 1999 poses were analyzed for each enzyme with substrate **2a**. The displayed poses were selected as corresponding to activity based on the similarity with the previously determined active pose of the natural substrate and the preservation of the experimentally observed stereoselectivity (Fig. 2C).[20] The correlation of the pose clusters with the calculated binding energy and distance from the cofactor supported the choice (full analysis in the ESI,† Fig. S2 and S3). The residue in position 166 is highlighted in red.

This allows for a more relaxed substrate conformation within the catalytic site, accommodating the carbamate and supporting the interaction with the catalytic Y128 for the activation of the indole ring. Our previous molecular dynamics simulation study on PsmD_*Sg* suggested that the W33–W166 interaction could be involved in the exit of the product after methylation, opening a channel between the connected α-helices.[20] Replacing residue W166 could also presumably affect the dynamics of the cavity opening, influencing the overall reaction rate.

Preparative enzymatic methylation of 2a

The best mutant, W166C, was used to obtain the product **2b** in a preparative manner, starting with 50 mg substrate, using a halide methyl transferase (*Ct*HMT) for the recycling of the SAM cofactor. The enzymes containing His-tags were immobilized on Ni-NTA resin and incubated in the presence of MeI, SAH and substrate **2a** (Fig. 7). This set-up was successfully used before for the preparative enzymatic methylation using StspM1 using the HMT-based cofactor recycling.[34] In this system, immobilized mutant W166C lead to product **2b** with 65% conversion after 20 h and 60% yield after purification by column chromatography.

Library generation and screening using substrate 3a

We chose to perform a limited screening for substrate **3a** due to its low solubility in the reaction medium. As such, we attempted a trial screen of three libraries: the randomized positions 33 and 166, as well as the combination between the two. We adapted the colorimetric assay by diluting the reaction sample with isopropanol to a 1 : 1 ratio, to address the substrate's poor solubility in water. This improved the detection of the substrate and allowed us to compare the absorbance at 580 nm within the wells of the reaction plates. Nevertheless, the assay sensitivity decreased substantially compared to the screening of compound **2a**, which could affect the detection of the poorer-performing mutants. However, we could identify hits in one of the three libraries, which upon further testing, performed better than the wild type in reaction with compound **3a**. Saturation mutagenesis in position 33 did not lead to any detectable hit. Interestingly, similarly to our previous screening with compound **2a**, the mutation of W166, this time to proline, provided a significant improvement in activity towards substrate **3a** (Fig. 8A). Starting with almost no activity of the wild type towards substrate **3a**, W166P increased the specific activity 28-fold. Although the activity towards compound **3a** needs further improvement for an efficient biocatalytic production of the phenserine precursor **3b**, we found that position 166 plays a key role, and further modifications could be considered for its surroundings. The double mutant

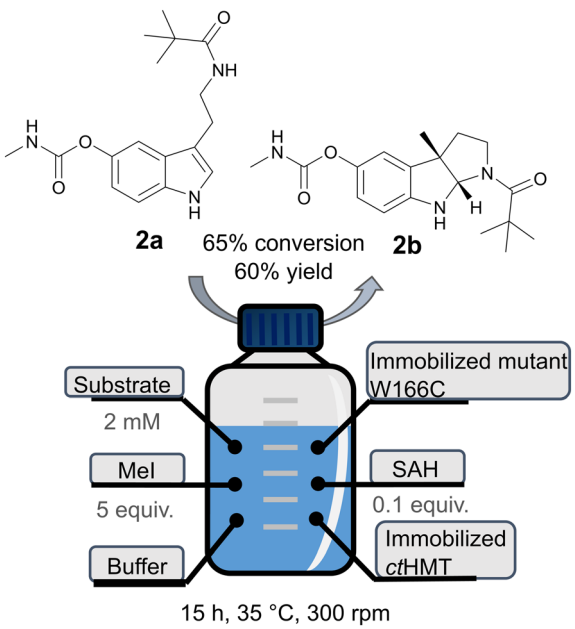

Fig. 7 Scheme of the procedure for the preparative enzymatic methylation of **2a** using the immobilized W166C mutant and the HMT-based cofactor recycling system.

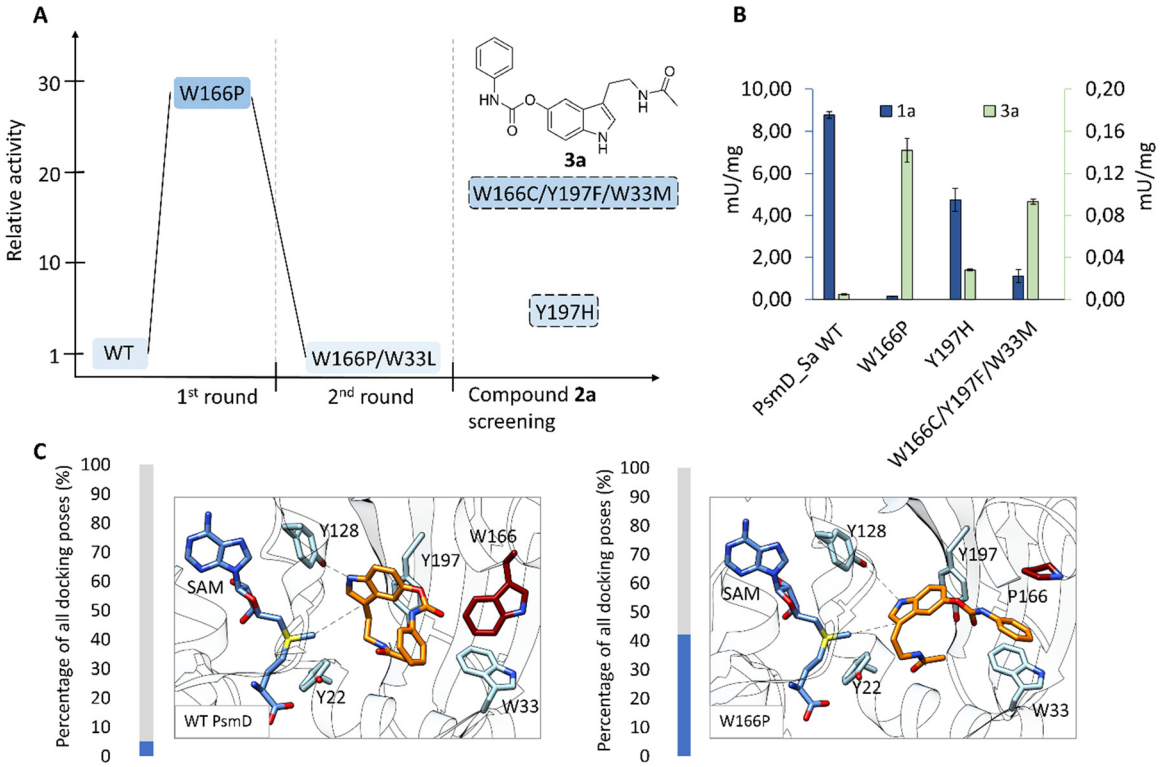

Fig. 8 A. Results of saturation mutagenesis screening rounds using **3a** as substrate. B. Specific activity of hit mutants towards **1a** (blue, left axis) and **3a** (green, right axis), compared to WT PsmD_*Sa*. C. Comparison of the docked active pose of substrate **3a** in the catalytic pocket of WT PsmD and mutant W166P. The proportion of the active binding mode in all the obtained docking poses is represented as percentages (blue). 1861 poses were analyzed for WT PsmD with substrate **3a** and 1791 poses for W166P. The displayed poses were selected as corresponding to activity based on the similarity with the previously determined active pose of the natural substrate.[20] The correlation of the poses with the calculated binding energy and distance from the cofactor supported the choice (full analysis in the ESI;† Fig. S4 and S5). The residue in position 166 is highlighted in red.

W166P/W33L, although identified as hit in the high-throughput assay, displayed no detectable activity towards substrate **3a** when isolated.

Given the uncertain positioning of the substrate in the catalytic pocket, we explored the idea that the hits identified in both screenings could also catalyse the reaction with the respective complementary substrate. To quantify their specific activity, we isolated and tested all the hits with both substrates using the MTase-Glo™ assay, which quantifies SAH production by converting it to ATP and measuring the luminescence in a luciferase reaction.[67] Interestingly, two hits from the substrate **2a** screening also show improved activity towards substrate **3a**. Y197H and the triple mutant W166C/Y197F/W33M increased the activity towards compound **3a** by 5- and 18-fold compared to the wild type (Fig. 8B).

An extensive docking approach was used for docking substrate **3a** into WT PsmD_*Sa* and the W166P variant, following the method described earlier. Molecular docking of **3a** into the W166P homology model (Fig. 8C) reveals a pose similar to that obtained for substrate **2a** in the W166C variant (Fig. 6), as well as the active pose of **1a** in WT (Fig. 2C and D). The mutation in position 166 promotes a relaxed conformation of the substrate, with the carbamate sidechain extending into the gap between W33 and P166. The π-stacking of the phenyl ring of the substrate with W33 could additionally stabilize the enzyme-substrate complex. When testing variants W166C and W166P with the other respective substrates, the results showed that the beneficial effects of the mutations are largely specific to the screened substrate. While variant W166C provided a 3-fold increase in activity towards substrate **3a**, compared to the WT, variant W166P led to a loss in activity towards substrate **2a** (Fig. S14†). The observed effect of mutations to residue W166 indicates its importance in substrate binding and enzyme selectivity. Further engineering approaches for other substrates substituted on the amide or carbamate side could benefit from addressing this position. The further evolution potential of this enzyme type might be worth exploring in relation to this site.

Conclusions

The use of an automated screening strategy allowed for the identification of multiple PsmD mutants displaying activity towards substrates with expanded non-polar functionalities, known to display AChE inhibition. Although methyltransferase engineering instances are relatively rare in literature, expanding the portfolio of successful examples

highlights the potential of engineering this class of enzymes in order to provide valuable routes in the synthesis of complex natural products and pharmaceuticals.

Data availability

The data supporting this article have been included as part of the ESI.†

Author contributions

DAA – conceptualization, data curation, formal analysis, investigation, methodology, validation, visualisation, writing – original draft. JT – data curation, formal analysis, investigation, methodology. TC – formal analysis, methodology. BD – formal analysis, methodology. TMR – methodology. HG, SN – project administration, supervision, resources. JP – conceptualization, funding acquisition, project administration, supervision, resources. All authors contributed to writing – review & editing.

Conflicts of interest

There are no conflicts to declare.

Acknowledgements

We gratefully acknowledge the German Federal Ministry of Education of Research (BMBF, "Modellregion, BioRevierPlus: BioökonomieREVIER Innovationscluster Biotechnologie & Kunststofftechnik-BioTech", grant number 031B1134A), as well as the Heinrich Heine University Düsseldorf and the Forschungszentrum Jülich GmbH for their ongoing support.

Notes and references

1 K. L. Davis, R. C. Mohs, J. R. Tinklenberg, A. Pfefferbaum, L. E. Hollister and B. S. Koppel, *Science*, 1978, **201**, 272–274.
2 D. J. Triggle, J. M. Mitchell and R. Filler, *CNS Drug Rev.*, 1998, **4**, 87–136.
3 A. Galli, G. Renzi, E. Grazzini, R. Bartolini, P. Aiello-Malmberg and A. Bartolini, *Biochem. Pharmacol.*, 1982, **31**, 1233–1238.
4 A. Kadir, N. Andreasen, O. Almkvist, A. Wall, A. Forsberg, H. Engler, G. Hagman, M. Lärksäter, B. Winblad, H. Zetterberg, K. Blennow, B. Långström and A. Nordberg, *Ann. Neurol.*, 2008, **63**, 621–631.
5 Q. Yu, C. Liu, M. Brzostowska, L. Chrisey, A. Brossi, N. Greig, J. R. Atack, T. T. Soncrant, S. I. Rapoport and H. Radunz, *Helv. Chim. Acta*, 1991, **74**, 761–766.
6 N. Canal and B. P. Imbimbo, *Clin. Pharmacol. Ther.*, 1996, **60**, 218–228.
7 M. A. Kamal, A. A. Al-Jafari, Q.-S. Yu and N. H. Greig, *Biochim. Biophys. Acta, Gen. Subj.*, 2006, **1760**, 200–206.
8 P. Schneider, B. Henßen, B. Paschold, B. P. Chapple, M. Schatton, F. P. Seebeck, T. Classen and J. Pietruszka, *Angew. Chem., Int. Ed.*, 2021, **60**, 23412–23418 (*Angew. Chem.*, 2021, **133**, 23600–23606).
9 T. A. Amador, L. Verotta, D. S. Nunes and E. Elisabetsky, *Planta Med.*, 2000, **66**, 770–772.
10 M. A. Schallenberger, T. Newhouse, P. S. Baran and F. E. Romesberg, *J. Antibiot.*, 2010, **63**, 685–687.
11 E. Viziteu, C. Grandmougin, H. Goldschmidt, A. Seckinger, D. Hose, B. Klein and J. Moreaux, *Br. J. Cancer*, 2016, **114**, 519–523.
12 Q.-s. Yu, X.-F. Pei, H. W. Holloway, N. H. Greig and A. Brossi, *J. Med. Chem.*, 1997, **40**, 2895–2901.
13 J. C. Yi, C. Liu, L. X. Dai and S. L. You, *Chem. – Asian J.*, 2017, **12**, 2975–2979.
14 T. Matsuura, L. E. Overman and D. J. Poon, *J. Am. Chem. Soc.*, 1998, **120**, 6500–6503.
15 T. Bui, S. Syed and C. F. Barbas, *J. Am. Chem. Soc.*, 2009, **131**, 8758–8759.
16 A. Pinto, Y. Jia, L. Neuville and J. Zhu, *Chem. – Eur. J.*, 2007, **13**, 961–967.
17 A. Huang, J. J. Kodanko and L. E. Overman, *J. Am. Chem. Soc.*, 2004, **126**, 14043–14053.
18 C. Sun, W. Tian, Z. Lin and X. Qu, *Nat. Prod. Rep.*, 2022, **39**, 1721–1765.
19 J. Liu, T. Ng, Z. Rui, O. Ad and W. Zhang, *Angew. Chem., Int. Ed.*, 2014, **53**, 136–139 (*Angew. Chem.*, 2014, **126**, 140–143).
20 D. A. Amariei, N. Pozhydaieva, B. David, P. Schneider, T. Classen, H. Gohlke, O. H. Weiergräber and J. Pietruszka, *ACS Catal.*, 2022, **12**, 14130–14139.
21 S. E. O'Connor, *Annu. Rev. Genet.*, 2015, **49**, 71–94.
22 A. Bar-Even and D. Salah Tawfik, *Curr. Opin. Biotechnol.*, 2013, **24**, 310–319.
23 C. Zeymer and D. Hilvert, *Annu. Rev. Biochem.*, 2018, **87**, 131–157.
24 M. T. Reetz and J. D. Carballeira, *Nat. Protoc.*, 2007, **2**, 891–903.
25 R. M. P. Siloto and R. J. Weselake, *Biocatal. Agric. Biotechnol.*, 2012, **1**, 181–189.
26 Y. Wang, P. Xue, M. Cao, T. Yu, S. T. Lane and H. Zhao, *Chem. Rev.*, 2021, **121**, 12384–12444.
27 N. J. Turner, *Nat. Chem. Biol.*, 2009, **5**, 567–573.
28 H. L. Schubert, R. M. Blumenthal and X. Cheng, *Trends Biochem. Sci.*, 2003, **28**, 329–335.
29 M. R. Bennett, S. A. Shepherd, V. A. Cronin and J. Micklefield, *Curr. Opin. Chem. Biol.*, 2017, **37**, 97–106.
30 D. Aynetdinova, M. C. Callens, H. B. Hicks, C. Y. X. Poh, B. D. A. Shennan, A. M. Boyd, Z. H. Lim, J. A. Leitch and D. J. Dixon, *Chem. Soc. Rev.*, 2021, **50**, 5517–5563.
31 H. Schönherr and T. Cernak, *Angew. Chem., Int. Ed.*, 2013, **52**, 12256–12267 (*Angew. Chem.*, 2013, **125**, 12480–12492).
32 E. Abdelraheem, B. Thair, R. F. Varela, E. Jockmann, D. Popadić, H. C. Hailes, J. M. Ward, A. M. Iribarren, E. S. Lewkowicz, J. N. Andexer, P. L. Hagedoorn and U. Hanefeld, *ChemBioChem*, 2022, **23**, e202200212.
33 B. J. C. Law, A.-W. Struck, M. R. Bennett, B. Wilkinson and J. Micklefield, *Chem. Sci.*, 2015, **6**, 2885–2892.

34 M. Haase, B. David, B. Paschold, T. Classen, P. Schneider, N. Pozhydaieva, H. Gohlke and J. Pietruszka, *ACS Catal.*, 2024, **14**, 227–236.
35 A. Gutmann, M. Schiller, M. Gruber-Khadjawi and B. Nidetzky, *Org. Biomol. Chem.*, 2017, **15**, 7917–7924.
36 E. Abdelraheem, E. Jockmann, J. Li, S. Günther, J. N. Andexer, P. L. Hagedoorn and U. Hanefeld, *ChemCatChem*, 2023, **16**, e202301217.
37 R. Roddan, F. Subrizi, J. Broomfield, J. M. Ward, N. H. Keep and H. C. Hailes, *Org. Lett.*, 2021, **23**, 6342–6347.
38 J. Fricke, A. Sherwood, R. Kargbo, A. Orry, F. Blei, A. Naschberger, B. Rupp and D. Hoffmeister, *ChemBioChem*, 2019, **20**, 2824–2829.
39 H. Stecher, M. Tengg, B. J. Ueberbacher, P. Remler, H. Schwab, H. Griengl and M. Gruber-Khadjawi, *Angew. Chem., Int. Ed.*, 2009, **48**, 9546–9548 (*Angew. Chem.*, 2009, **121**, 9710–9712).
40 E. Jockmann, F. Subrizi, M. K. F. Mohr, E. M. Carter, P. M. Hebecker, D. Popadić, H. C. Hailes and J. N. Andexer, *ChemCatChem*, 2023, **15**, e202300930.
41 S. Mordhorst, J. Siegrist, M. Müller, M. Richter and J. N. Andexer, *Angew. Chem., Int. Ed.*, 2017, **56**, 4037–4041 (*Angew. Chem.*, 2017, **129**, 4095–4099).
42 C. Liao and F. P. Seebeck, *Nat. Catal.*, 2019, **2**, 696–701.
43 S. Mordhorst and J. N. Andexer, *Nat. Prod. Rep.*, 2020, **37**, 1316–1333.
44 X. Wen, F. Leisinger, V. Leopold and F. P. Seebeck, *Angew. Chem., Int. Ed.*, 2022, **61**, e202208746 (*Angew. Chem.*, 2022, **134**, e202208746).
45 D. Popadić, D. Mhaindarkar, M. H. N. Dang Thai, H. C. Hailes, S. Mordhorst and J. N. Andexer, *RSC Chem. Biol.*, 2021, **2**, 883–891.
46 G.-Y. Yang, G.-W. Zheng, B.-B. Zeng, J.-H. Xu and Q. Chen, *Mol. Catal.*, 2023, **550**, 113533.
47 X. Wang, C. Wang, L. Duan, L. Zhang, H. Liu, Y.-m. Xu, Q. Liu, T. Mao, W. Zhang, M. Chen, M. Lin, A. A. L. Gunatilaka, Y. Xu and I. Molnár, *J. Am. Chem. Soc.*, 2019, **141**, 4355–4364.
48 B. Aberle, D. Kowalczyk, S. Massini, A. N. Egler-Kemmerer, S. Gergel, S. C. Hammer and B. Hauer, *Angew. Chem., Int. Ed.*, 2023, **62**, e202301601 (*Angew. Chem.*, 2023, **135**, e202301601).
49 A. Kunzendorf, B. Zirpel, L. Milke, J. P. Ley and U. T. Bornscheuer, *ChemCatChem*, 2023, **15**, e202300951.
50 Q. Tang, C. W. Grathwol, A. S. Aslan-Üzel, S. Wu, A. Link, I. V. Pavlidis, C. P. S. Badenhorst and U. T. Bornscheuer, *Angew. Chem., Int. Ed.*, 2021, **60**, 1524–1527 (*Angew. Chem.*, 2021, **133**, 1547–1551).
51 K. H. Schulke, J. S. Frose, A. Klein, M. Garcia-Borras and S. C. Hammer, *ChemBioChem*, 2024, e202400079.
52 C. Y. Gao, G. Y. Yang, X. W. Ding, J. H. Xu, X. Cheng, G. W. Zheng and Q. Chen, *Angew. Chem., Int. Ed.*, 2024, **63**, e202401235 (*Angew. Chem.*, 2024, **136**, e202401235).
53 S. Ju, K. P. Kuzelka, R. Guo, B. Krohn-Hansen, J. Wu, S. K. Nair and Y. Yang, *Nat. Commun.*, 2023, **14**, 5704.
54 L. L. Bengel, B. Aberle, A. N. Egler-Kemmerer, S. Kienzle, B. Hauer and S. C. Hammer, *Angew. Chem., Int. Ed.*, 2021, **60**, 5554–5560 (*Angew. Chem.*, 2021, **133**, 5614–5620).
55 W. Butdee, S. Muangham, D. Chonudomkul and K. Duangmal, *Int. J. Syst. Evol. Microbiol.*, 2023, **73**, 005639.
56 Q.-s. Yu, H. W. Holloway, J. L. Flippen-Anderson, B. Hoffman, A. Brossi and N. H. Greig, *J. Med. Chem.*, 2001, **44**, 4062–4071.
57 J. Klein, *Expert Opin. Invest. Drugs*, 2007, **16**, 1087–1097.
58 S. Barik, *Int. J. Mol. Sci.*, 2020, **21**, 8776.
59 K. Świderek, I. Tuñón, I. H. Williams and V. Moliner, *J. Am. Chem. Soc.*, 2018, **140**, 4327–4334.
60 R. J. Boyd, C. K. Kim, Z. Shi, N. Weinberg and S. Wolfe, *J. Am. Chem. Soc.*, 1993, **115**, 10147–10152.
61 J. Zhang, H. J. Kulik, T. J. Martinez and J. P. Klinman, *Proc. Natl. Acad. Sci. U. S. A.*, 2015, **112**, 7954–7959.
62 J. Zhang and J. P. Klinman, *J. Am. Chem. Soc.*, 2016, **138**, 9158–9165.
63 S. Kille, C. G. Acevedo-Rocha, L. P. Parra, Z.-G. Zhang, D. J. Opperman, M. T. Reetz and J. P. Acevedo, *ACS Synth. Biol.*, 2013, **2**, 83–92.
64 T. M. Rosch, J. Tenhaef, T. Stoltmann, T. Redeker, D. Kosters, N. Hollmann, K. Krumbach, W. Wiechert, M. Bott, S. Matamouros, J. Marienhagen and S. Noack, *ACS Synth. Biol.*, 2024, **13**, 2227–2237.
65 D. A. Amariei, M. Haase, M. K. T. Klischan, M. Wäscher and J. Pietruszka, *ChemCatChem*, 2024, e202400052.
66 B. Webb and A. Sali, *Curr. Protoc. Bioinf.*, 2016, **54**, 5.6.
67 K. Hsiao, H. Zegzouti and S. A. Goueli, *Epigenomics*, 2016, **8**, 321–339.

